Allergologia et immunopathologia
Sociedad Española de Inmunología Clínica, Alergología y Asma Pediátrica
www.all-imm.com

RESEARCH ARTICLE

OPEN ACCESS

Whole-exome sequencing identified a homozygous novel *RAG1* mutation in a child with omenn syndrome

Wendi Wang[a†], Jian Wang[a†], Jingjing Wang[a], Jingting Liu[a], Jianying Pei[a], Wanyi Li[a], Yanxia Wang[a], Santasree Banerjee[b], Ruifeng Xu[a*], Zhaoyan Meng[a*], Bin Yi[a*]

[a]*Gansu Provincial Maternity and Child-Care Hospital, 143, North Street, Qilihe District, Lanzhou, Gansu Province 730050, China*
[b]*Department of Genetics, College of Basic Medical Sciences, Jilin University, Changchun, China*

[†]*The authors contributed equally to the work.*

Received 24 October 2021; Accepted 13 June 2022
Available online 1 November 2022

KEYWORDS
frameshift mutation;
immune responses;
omenn syndrome;
RAG1 gene;
SCID

Abstract
Introduction and objectives: Omenn syndrome (OS) is a very rare type of severe combined immunodeficiencies manifested with erythroderma, eosinophilia, hepatosplenomegaly, lymphadenopathy, and elevated level of serum IgE. OS is inherited with an autosomal recessive mode of inheritance. Germline mutations in the human *RAG1* gene cause OS.
Materials and methods: In this study, we investigated a 2-month-old boy with cough, mild anaemia, pneumonia, immunodeficiency, repeated infection, feeding difficulties, hepatomegaly, growth retardation, and heart failure. Parents of the proband were phenotypically normal.
Results: Karyotype analysis and chromosomal microarray analysis found no chromosomal structural abnormalities (46, XY) and no pathogenic copy number variations (CNVs) in the proband. Whole-exome sequencing identified a novel homozygous single nucleotide deletion (c.2662delC) in exon 2 of the *RAG1* gene in the proband. Sanger sequencing confirmed that both the proband parents were carrying this variant in a heterozygous state. This variant was not identified in two elder sisters and one elder brother of the proband and in the 100 ethnically matched normal healthy individuals. This novel homozygous deletion (c.2662delC) leads to the frameshift, which finally results in the formation of the truncated protein (p.Leu888Phefs*3) V(D)J recombination-activating protein 1 with 890 amino acids compared with the wildtype V(D)J recombination-activating protein 1 of 1043 amino acids. Hence, it is a *loss-of-function* variant.
Conclusions: Our present study expands the mutational spectrum of the *RAG1* gene associated with OS. We also strongly suggested the importance of whole-exome sequencing for the genetic screening of patients with OS.

***Corresponding authors:** Dr. Ruifeng Xu, Gansu Provincial Maternity and Child-Care Hospital, 143 North Street Qilihe District, Lanzhou, Gansu Province 730050, China. *Email address*: 1469535177@qq.com; Dr. Zhaoyan Meng, Gansu Provincial Maternity and Child-Care Hospital, 143 North Street Qilihe District, Lanzhou, Gansu Province 730050, China. *Email address*: 540486046@qq.com; Dr. Bin Yi, Gansu Provincial Maternity and Child-Care Hospital, 143 North Street Qilihe District, Lanzhou, Gansu Province 730050, China. *Email address*: www.0931@163.com

https://doi.org/10.15586/aei.v50i6.529

Introduction

Human severe combined immunodeficiency (SCID) is a large group of genetic disorders with extreme genotypic and phenotypic heterogeneity.[1] SCID is usually characterized by severe, recurrent, and potentially lethal infections that occur soon after birth or early in infancy. Patients with SCID usually manifest with failure to thrive and lymphopenia of T lymphocytes.[2] SCID patients also presented with a deficiency of antibodies and complete loss or marked abnormalities in cell-mediated immunity.[3] SCID patients were classified into two types based on the presence (B^+ SCID) or absence (B^- SCID) of B cells in the peripheral blood.[4,5]

Omenn syndrome (OS) is a very rare type of inherited SCID presented with several early postnatal or infancy onset manifestations, i.e., diffuse exfoliative erythroderma, lymphadenopathy, hepatosplenomegaly protracted diarrhoea, alopecia, failure to thrive, eosinophilia, elevated level of serum immunoglobulin E (IgE) with typical recurrent severe life-threatening infections.[6] Laboratory investigations of SCID patients usually showed eosinophilia and T-cell lymphocytosis.[7] According to immunological phenotypes, OS is classified into two types, namely $T^+B^-NK^+$ and $T^-B^-NK^+$.[8] To date, OS could only be treated by bone marrow transplantation or cord blood stem cell transplantation.[8]

Germline mutations in recombination-activating genes 1 (*RAG1*) cause the majority of OS.[9] *RAG1* gene is located at the short arm of chromosome 11 (11p12). *RAG1* gene encodes a lymphoid-specific complex of enzymes named V(D)J recombination-activating protein 1. This protein plays a significant role in initiating the V(D)J recombination process.[10] During the development of T-cell and B-cell receptors, V(D)J recombination-activating protein 1 is involved in the process of rearrangement of the variable (V), diversity (D), and joining (J) segments. Both RAG1 and RAG2 proteins combined and cleaved the recombination signal sequences (RSSs), variable (V), diversity (D), and joining (J) gene exons and initiating the recombination process of variable (V), diversity (D), and joining (J) segments. This process of somatic recombination leads to the formation of diverse T-cell and B-cell repertoires.[11] Germline mutations in *RAG1* genes causes complete loss or reduced recombination V(D) J followed by the loss of the development of both B and T cell, which finally results in the deficiency of circulating B cells and non-functional oligoclonal T cells, leads to severe combined immunodeficiency (SCID).[12,13] In addition, *RAG1* hypomorphic mutations lead to the formation of partially functional RAG1 protein followed by the partial development of B and T lymphocytes which in turn causes phenotypic heterogeneity and a spectrum of severe immunodeficiencies.[14,15] According to the different levels of RAG1 expression, patients with OS showed a spectrum of immunological phenotypes and diverse clinical manifestations.[16]

Here, we presented the case of a 2-month-old patient clinically diagnosed with OS. Karyotype and chromosomal microarray analyses found no chromosomal structural abnormality in the proband (46, XY) and did not identify any pathogenic copy number variations (CNVs) in the chromosomes of the proband. Whole-exome sequencing (WES) identified a novel homozygous deletion (c.2662delC) in exon 2 of the *RAG1* in the proband. Sanger sequencing confirmed that both the proband parents were carrying this variant in a heterozygous state. This variant leads to the truncated RAG1 (p.Leu888Phefs*3) protein with 890 amino acids compared with the wildtype RAG1 protein of 1043 amino acids. Our present study expands the mutational spectrum of the RAG1 gene associated with OS. We also strongly suggested the application of WES for accurate, timely, and cost-effective screening for patients with OS.

Materials and Methods

Patient and clinical samples

A Hui Chinese infant with OS was enrolled in our hospital (Gansu Provincial Maternity and Child-Care Hospital, Lanzhou, Gansu Province, People's Republic of China). Blood samples were collected for analysis. The study was approved by the ethics committee of our hospital (Gansu Provincial Maternity and Child-Care Hospital, Lanzhou, Gansu Province, People's Republic of China), following the Declaration of Helsinki guidelines. We obtained written informed consent from all of the participants of this study.

Karyotype and chromosomal microarray analyses

We performed standard G-banding karyotyping to analyse the structure of all chromosomes in the proband. Next, to confirm the presence of copy number variations (CNV) in the proband, chromosome microarray analysis was performed using a CytoScan HD array (Affymetrix), according to the manufacturer's protocols (Affymetrix). Chromosome Analysis Suite software version 1.2.2 was used for analysing the data. The reporting threshold of copy number was set at 10 kb with the marker count ≥50.[17]

Whole-exome sequencing

Blood samples were collected and genomic DNA was extracted from proband using a QIAamp DNA Blood Mini Kit (Qiagen, Hilden, Germany) following the manufacturer's instructions. Proband's genomic DNA was subjected to WES. Agilent SureSelect version 6 (Agilent Technologies, Santa Clara, CA) was used for capturing sequences. Then, the enriched library was sequenced on an Illumina HighSeq4000. Next, WES reads were aligned to the GRCh37.p.10 by using Burrows–Wheeler Aligner software (version 0.59). After that, GATK IndelRealigner was used for local realignment of the Burrows–Wheeler aligned reads. Then, the base quality recalibration of the Burrows–Wheeler aligned reads was performed by using the GATK Base Recalibrator. Next, the identification of single-nucleotide variants (SNV) and insertions or deletions (indel) was done by the GATK Unified Genotyper. Then, variants were annotated with the Consensus Coding Sequences Database (20130630) at the National Center for Biotechnology Information. Illumina pipeline was used for image analysis and base calling. Indexed primers were used for data fidelity surveillance. In order to align the clean sequencing reads with the human reference genome (hg19), SOAP aligner (soap2.21) software

was used. Then, to assemble the consensus sequence and call genotypes in target regions, we used SOAPsnp (v1.05) software.

Bioinformatics analysis

Identified variants by WES were selected for data interpretation with minor allele frequency <0.01 in dbSNP, Hapmap, 1000 Genomes Project, and our in-house database for 5,000 Chinese. Data analysis was performed based on the variant interpretation guidelines of the American College of Medical Genetics and Genomics (ACMG).[18] Deleterious variations were selected and performed their segregation analysis among the family members. The variants' function and association with the disease phenotype was done based on the information from OMIM database and previously published literature.

Sanger sequencing

To validate the identified variants by WES, we performed Sanger sequencing. Designing primer pairs for the candidate loci have been done based on the reference genomic sequences of the Human Genome from GenBank in NCBI. Primer pairs were synthesized by Invitrogen, Shanghai, China. Polymerase chain reaction (PCR) was performed with an ABI 9700 Thermal Cycler. Next, directly sequenced the PCR products by an ABI PRISM 3730 automated sequencer (Applied Biosystems, Foster City, CA, USA). Analysis of sequencing data has been done by DNASTAR SeqMan (DNASTAR, Madison, Wisconsin, USA).

WES identified the novel homozygous variant, which was validated by Sanger sequencing using the following primers: F1 5′-GGCGCGGGGGTCTCGCGGCG-3′, R1 5′-GGCGGCGAATTCTATAGCG-3′. The reference sequence NM_000448.2 of *RAG1* was used.

In silico analysis

The variant identified in the proband by WES was analysed by Mutation Taster (http://mutationtaster.org/).[19]

Data availability

All data used for the analyses in this report supporting the findings of this study are available on reasonable request to the corresponding author.

Results

Human subjects

We investigated a proband of a nonconsanguineous Hui Chinese family. He was the fourth child in his family. He was born after full-term delivery, weighing 3.3 kg and showed normal breastfeeding after birth. The child has two elder sisters and one elder brother who are in good health. No history of genetic and metabolic diseases was found in his family Figure 1.

At the age of one month, the child developed coughing, 2-3 sounds/burst, less sputum without wheezing, fever, and hoarseness. He was first admitted to a local hospital and given intravenous infusion (specifically unknown) for 10 days. After that, the proband has been suffering from frequent coughing with bruising around the mouth. He was then admitted to our hospital (Gansu Provincial Maternity and Child-Care Hospital) for intravenous infusion (specifically unknown), and his cough was relieved. Then, he was again admitted to our hospital with coughing accompanied by occasional bruising around the mouth and changes in stool characteristics. However, we have not found the obvious cause of recurrence of frequent coughing in this proband. There was no fever, no breathing difficulties or other symptoms manifested in the proband.

Physical examination revealed that his body temperature was 36.9°C, pulse rate was 170 beats/min, breath rate was 84/min, blood pressure was 87/47 mmHg and body weight was 5.28 kg with 90% SpO_2.

The proband clinically manifested normal development, malnutrition, drowsiness, poor mental response and normal skin colour with decreased elasticity. The proband was characterized by dry lips and red throat, and the pharynx was slightly congested with copious white secretions, which could be seen on both sides of the oral mucosa and the isthmus, easy to peel and easy to exfoliate. The proband was identified with normal head size with Bregma Depression size of 3.0 × 3.0 cm^2. No visual or hearing impairments were found in the proband. The proband presented with thick breath sounds in both lungs with normal breathing movements, strong heart sounds with a heart rate of 170 beats/min, normal rhythm and no murmurs. Normal abdominal appearance with a soft belly, 4.5 cm below the liver ribs palpable, and active bowel sounds were reported. The proband's gallbladder, spleen and kidneys were normal. The proband's lymph nodes were normal, and superficial lymph nodes were present throughout the body without any swelling. We identified no abnormal vascular signs in the peripheral blood vessels and no neuromuscular abnormalities in the proband. During the course of the illness, the proband's mental state was slightly worse. The proband was manifested with poor appetite but without vomiting and diarrhoea.

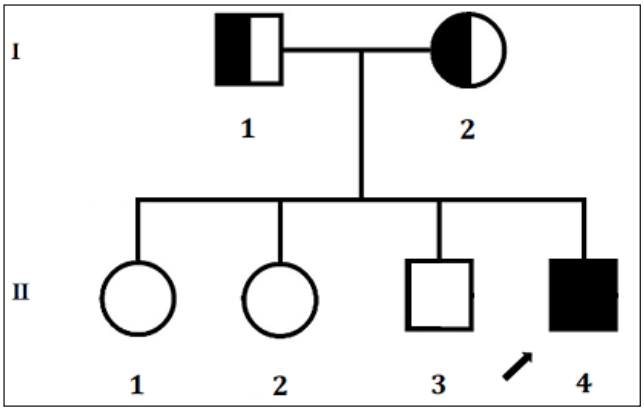

Figure 1 Pedigree of the Chinese family with OS. Squares and circles denoted males and females respectively. Individuals labelled with a solidus were deceased. Roman numerals indicate generations. Arrow indicates the proband (II-4).

In the proband, we found that the colour Doppler of two-dimensional and M-type Doppler measurements (mm) was AO 9 LA 14 IVS 3 LV 20/12 LVPW 3 RV 9 MPA 11 LPA 5 RPA 5 EF 70 (%) FS 40 (%) and Spectrum Doppler ultrasound (cm/s) was MV 85 TV 76 AV 102 PV 98.

The inner diameter of each chamber of the heart was normal. The interventricular septum was not thick. No echo of the arterial catheter was detected, and each valve's shape and opening and closing were normal. Left ventricular ejection fraction and short-axis contraction rate was in normal range. No abnormal blood flow signal and frequency spectrum were detected.

There was no obvious abnormality in the structure of the heart and blood flow. The left and right ventricular systolic and diastolic functions were normal. There was no obvious abnormality in pulmonary artery pressure.

The chest CT found that the chest was symmetrical with a centrally located trachea. The texture of the two lungs was increased, and the upper field mass flaky high-density shadow was visible in the inner area of the two lungs. The right edge was blurred. The diaphragm muscles were smooth on both sides, and the bilateral costal diaphragm angle was sharp. The proband was clinically diagnosed with "bronchial pneumonia" (Figure 2).

Later, we performed chest CT and identified that the end of the endotracheal tube was at the level of the lower edge of T1. Gradually, we found that the end of the endotracheal tube was at the level of the T1 vertebral body. Finally, we identified that the tip of the endotracheal tube was at the level of the T2 vertebral body. Hence, we clinically diagnosed the patient with severe pneumonia of the two lungs. Therefore, chest CT is recommended for further examination.

We identified mass-shaped high-density shadows on the right lung, and there were bronchial inflation shadows. Severe pneumonia in both of the lungs (Figure 2A). Compared with the previous film (2019-04-09), we found that the bipulmonary pneumonia had improved and better than before (Figure 2B). Compared with the previous film (2019-04-12), we identified that the bipulmonary pneumonia was heavier than before. The end of the endotracheal tube was at the level of the lower edge of T1 (Figure 2C). Compared with the previous film (2019-04-16), the bipulmonary pneumonia was heavier than before, and the tip of the endotracheal tube was at the level of the T1 vertebral body (Figure 2D). Compared with the previous film (2019-04-19), we found severe pneumonia of the two lungs was worse. Chest CT was recommended for further examination. The end of the endotracheal tube was at the level of the T2 vertebral body (Figure 2E).

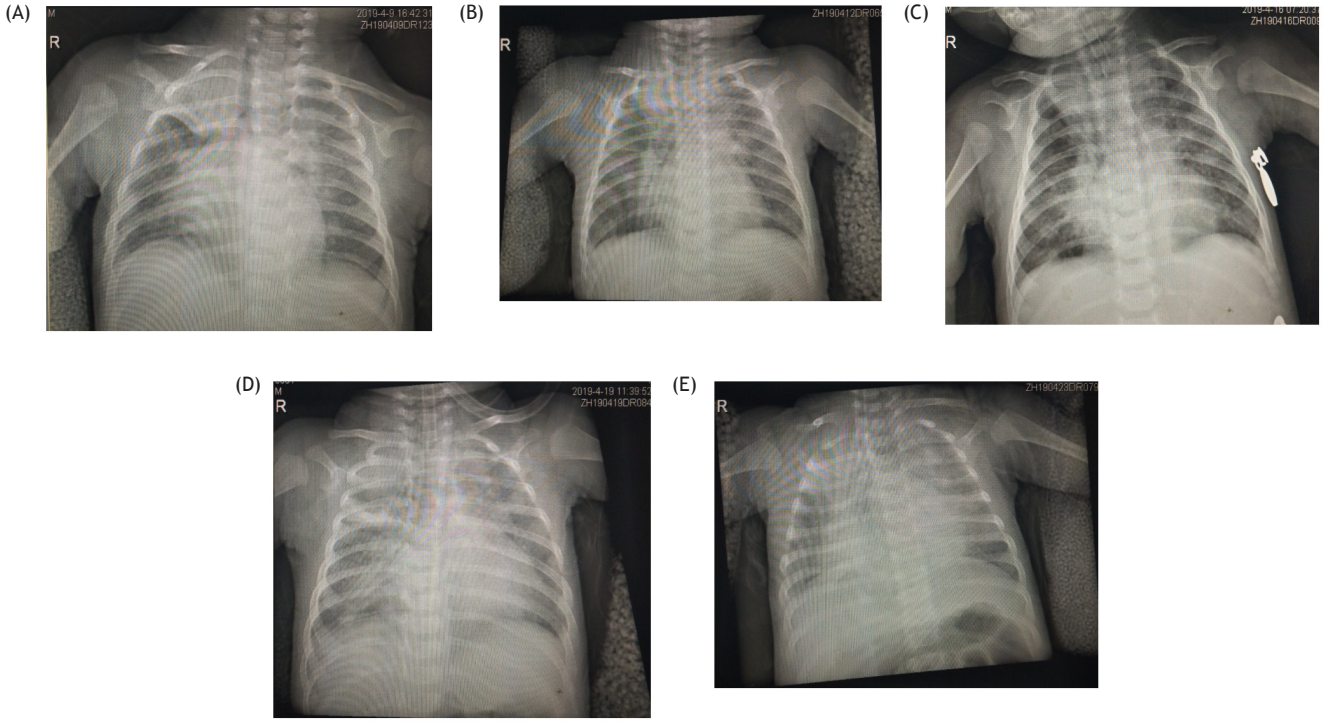

Figure 2 Chest CT examination. (A) The texture of the two lungs increased, with blurred edges. On the right lung, mass-shaped high-density shadows, and bronchial inflation shadows. Severe pneumonia in both lungs, the part of the right lung is actually changed. (B) The texture of the two lungs increased, and the flake high-density shadow and the right lung upper field mass flaky high-density shadow were visible in the inner area of the two lung fields, and the density was lighter. Bipulmonary pneumonia has absorbed and improved better than before. (C) The end of the endotracheal tube is at the level of the lower edge of T1. The double pneumonia is heavier than before. The end of the endotracheal tube is at the level of the lower edge of T1. (D) The tip of the endotracheal tube is at the level of the T1 vertebral body. The double pneumonia is heavier than before, the tip of the endotracheal tube is at the level of the T1 vertebral body. (E) The tip of the endotracheal tube is at the level of the T2 vertebral body. Severe pneumonia of the two lungs is worse than before, except for the limited consolidation. The end of the endotracheal tube is at the level of the T2 vertebral body

Laboratory findings

We performed routine blood tests, protein and enzymatic analyses, immunopathological analysis, amino acid analysis, clotting factor analysis, hepatitis antigen-antibody analysis, viral and bacterial studies, bacterial and fungal cultures, bacterial DNA study, cellular immunoassay, G-experiment, endotoxin test, blood grouping, physical and chemical characteristics of blood and urine and stool culture of the patient. The results of each test were given in detail (Supplementary Table S1-S14).

Immunological findings

FACS results showed that the percentages of T cells (patient: 0.00%; controls: 60.8-75.4%) and B cells (patient: 0.00%; controls: 6.0-25.0%) present in the proband were significantly lower than those from the healthy family members. The percentage of $CD3^{-}CD56^{+}$ NK cells were significantly higher (patient: 99.0%; controls: 5.0-20.0%). We further studied the subpopulation of T cells including CD4 and CD8. The percentage of CD4+ T cells (patient: 0.00%; controls: 29.4-45.8%) and CD8+ T cells (patient: 0.00%; controls: 18.2-32.8%) were significantly lower in the patient (Figure 3).

Immunoglobulin expression on B cells was also investigated. The levels of both IgA and IgM expression were considerably lower in the patient than in other healthy family members.

Whole-exome sequencing and Sanger sequencing identified a homozygous novel variant in RAG1

We performed WES of DNA from the proband. WES identified a novel homozygous single nucleotide deletion

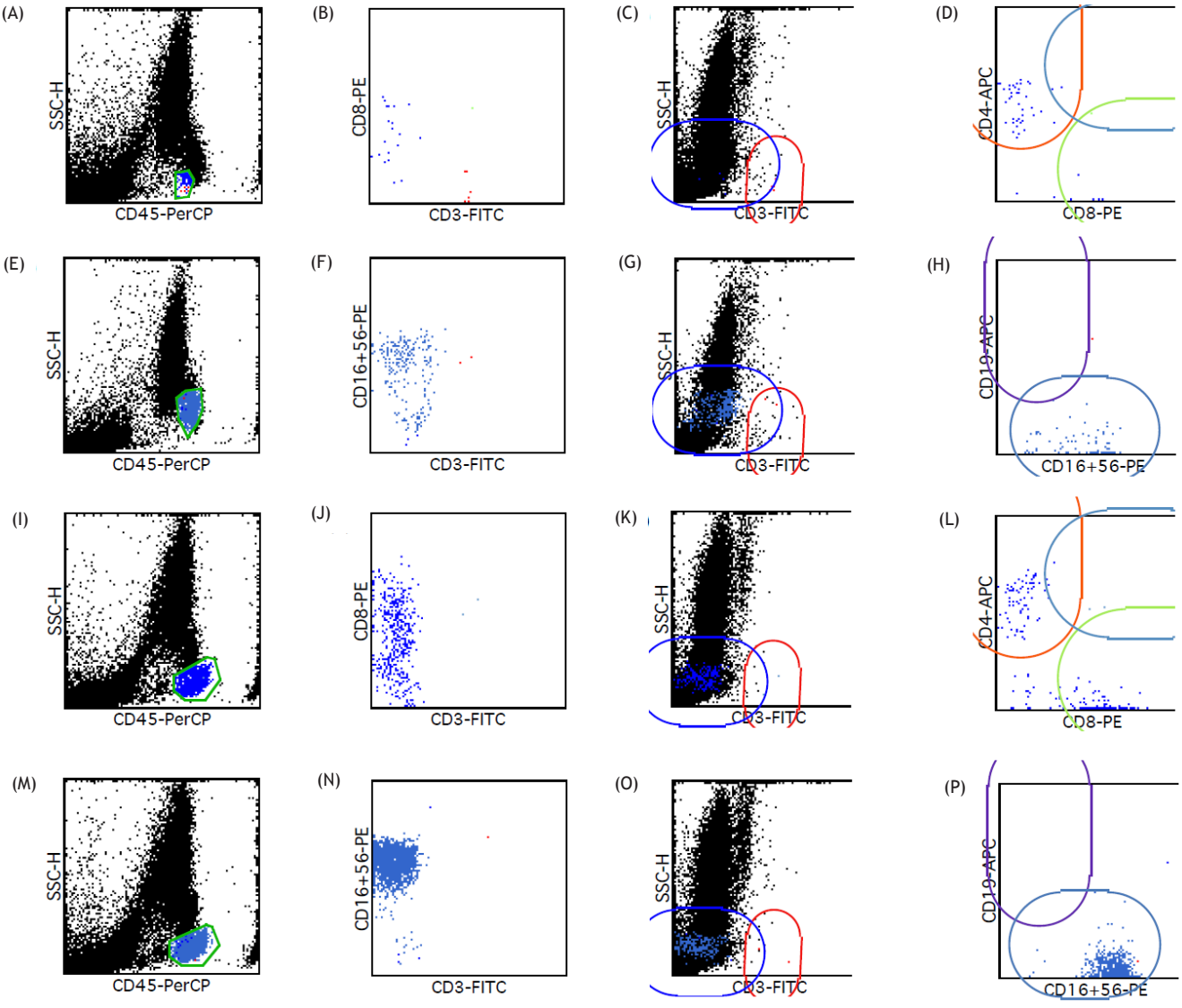

Figure 3 (A-P) FACS results showed that the percentages of T cells (patient: 0.00%; controls: 60.8-75.4%) and B cells (patient: 0.00%; controls: 6.0-25.0%) present in the patient were significantly lower than those from the family members. The percentage of $CD3^{-}CD56^{+}$ NK cells were significantly higher (patient: 99.0%; controls: 5.0-20.0%). The subpopulation of T cells including CD4 and CD8. The percentage of CD4+ T cells (patient: 0.00%; controls: 29.4-45.8%) and CD8+ T cells (patient: 0.00%; controls: 18.2-32.8%) were also affected in the patient.

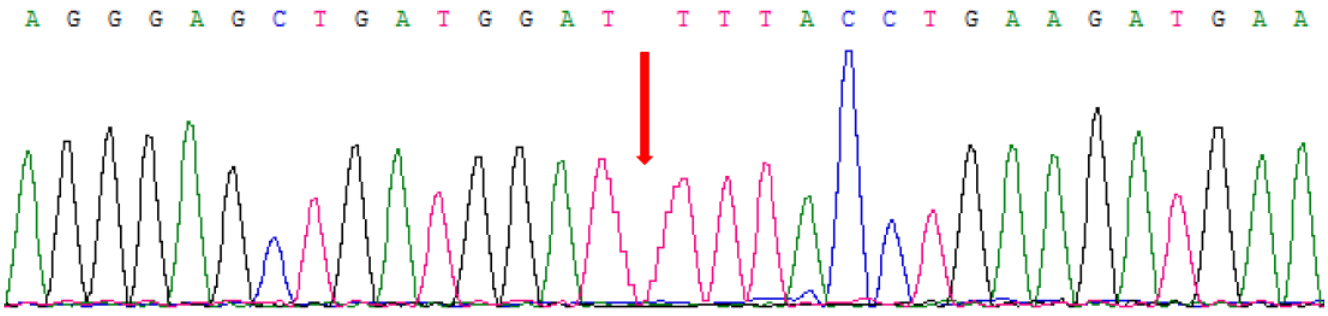

Figure 4 Partial DNA sequences in the *RAG1* gene by Sanger sequencing of the patient. The reference sequence NM_000448.2 of *RAG1* gene was used.

(c.2662delC), in exon 2 of the *RAG1* gene in the proband (Figure 4). This novel homozygous variant leads to a frameshift (p.Leu888Phefs*3) followed by premature translation termination, which finally results in the formation of a truncated RAG1 protein of 890 amino acids instead of the wild type RAG1 protein consisting of 1043 amino acids. Hence, it is a *loss-of-function* variant. Sanger sequencing confirmed that both the father and mother of the proband were harbouring this variant in a heterozygous state. Sanger sequencing also revealed that two elder sisters and one elder brother of the proband were phenotypically normal and lacked this variant. This variant is not found in 100 normal control individuals of the same ethnicity. This variant is also not present in the Human Gene Variant database (HGMD, www.hgmd.cf.ac.uk/), Online Mendelian Inheritance in Man (MIM, (https://www.omim.org). This homozygous novel variant is also not found in our in-house database, consisting of ~50,000 Chinese Han samples. We also did not find this variant in ExAC (exac.broadinstitute.org), gnomAD (https://gnomad.broadinstitute.org), dbSNP (https://www.ncbi.nlm.nih.gov/SNP) and 1000 Genome Database (www.internationalgenome.org).

In silico analysis

The variant (c.2662delC; p.L888Ffs*3) was predicted as "disease causing" by the Mutation Taster (http://mutationtaster.org/).[19]

Discussion

In 1965, OS was described and reported for the first time by Omenn, 1965.[20] Although, pathogenesis of OS is complex, germline mutations in *RAG1* gene is the genetic cause among most OS patients.[16] In the present study, we analysed and investigated the clinical, immunological, and genetic characteristics of one patient with OS in our hospital. The affected child was carrying a frameshift mutation (c.2662delC, p.Leu888Phefs*3) in exon 2 of the *RAG1* gene. This mutation was predicted to be deleterious and disease-causing. Furthermore, this novel frameshift mutation induced a premature stop codon and led to the formation of a truncated RAG1 protein.

RAG1 gene is significantly involved in the initiation of recombination process of the V, (D), and J segments, which finally form the variable portions of immunoglobulin and TCR proteins.[9] Germline mutations in *RAG1* gene causes profound reduction of T and B cells, leads to the occurrence of OS.[1] OS is extremely rarest types of SCID, usually manifested with gradually and progressively increased oligoclonal and activated T cells, with absence of B lymphocytes, which in turn results into the clinical phenotype including generalized erythroderma, lymphadenopathy, hepatosplenomegaly, eosinophilia, and elevated level of serum IgE. Unlike most of the OS cases with easy clinical diagnosis, some cases of maternal T cells engraftment within the foetus are really challenging. Hence, clinical diagnosis and treatment of OS patients is highly challenging without proper genetic screening. In Chinese population, the incidence rate of OS is very rare and only one OS patient has been reported so far.[9] Here, we analysed and investigated the phenotype and genotype of a children with OS in a nonconsanguineous Chinese family.

To date, more than 50 variants of *RAG1* gene have been reported in *RAG1* mutation database (https://databases.lovd.nl/shared/variants/RAG1/unique?search_var_status=%3D%22Marked%22%7C%3D%22Public%22). Among these reported variants of the *RAG1* gene, most are null or loss-of-function mutations.[21] We reported a homozygous novel single nucleotide deletion in *RAG1* gene, which led to a frameshift followed by the formation of a truncated RAG1 protein. Interestingly, the same *RAG1* variants also cause different clinical manifestations.[22] The human *RAG1* is a highly conserved gene, homozygous or compound heterozygous mutation only causes OS in an autosomal recessive mode of inheritance. According to the information provided by GnomAD, only 44% of amino acids in RAG1 is reported to cause OS upon mutation. However, functional characterization of the reported variants was very challenging.[23] In addition, identifying variants based on low allele frequency is also not always correct since the *RAG1* gene is highly conserved. OS patients with germline mutations in *RAG1* gene usually presented with diverse phenotypes, and the treatment strategies are also highly variable among patients. Hematopoietic stem cell transplantation could be recommended for some OS patients, while mechanism-based treatment also became a good approach for other patient groups depending on their phenotypes.[24,25]

The patients with OS usually presented with decreased number of dysfunctional T cells, the complete absence of B cells, with normal counts of NK cells.[26] Therefore, OS

patients showed an immunological phenotype of $T^-B^-NK^+$. Additionally, patients with OS also manifested significantly increased eosinophil counts and elevated serum IgE levels.[27] Reduced or complete absence of both T and B cells leads to recurrent and severe infections in infancy for patients with OS. In patients with OS, loss of balance in the Th1/Th2 ratio causes increased secretion of IL-4 and IL-5 followed by elevated serum IgE levels, which finally results into eczema-like rashes.[28,29] However, due to dysfunctional T-cells, patients with OS are usually identified with monoclonal TCR peaks. Dysfunctional T-cells and dysplasia of B-cells lead to cellular and humoral immune system abnormalities in patients with OS. Treatment with gamma globulin or antibiotic administration was not adequate or effective for patients with OS.

OS is a very rare and extremely heterogeneous (both genotypically and phenotypically) disorder. Single-gene sequencing or targeted next-generation sequencing does not always identify the candidate variants in patients with OS.[30] Therefore, WES is more accurate and reliable for identifying the candidate gene and variants underlying the disease phenotype in patients with OS.[31] WES is one of the most significant technologies for identifying candidate gene and disease-causing variants in patients with OS.[32] WES is a more accurate, rapid and cost-effective tool for early and timely molecular genetic analysis allowing clinicians for making an accurate clinical diagnosis.[33,34] Our present study not only expands the mutational spectrum of the OS gene but also strongly emphasizes the significance of WES as an accurate, rapid and cost-effective tool for molecular genetic analysis for patients with OS.

Acknowledgements

We are thankful to the proband and all the family members for participating in our study. We also thankful to the Gansu Health Scientific Research Project (GSWSKY2017-22) and Gansu Provincial Key Laboratory of Birth Defect Prevention and Control Research (1506RTSA158).

Conflict of Interest

The authors confirm that there are no conflicts of interest.

Author Contributions

Designed the study: Bin Yi, Ruifeng Xu, Zhaoyan Meng and Santasree Banerjee. Conducted acquisition and analysis of all the clinical data: Wendi Wang, Jian Wang, Jingjing Wang. WES pipeline and analysed the data: Jingting Liu, Jianying Pei, Wanyi Li. Selected patients and performed WES: Jianying Pei, Wanyi Li, and Yanxia Wang. Supervised manuscript preparation and edited the manuscript: Wendi Wang, Jian Wang, Jingjing Wang, Ruifeng Xu, Zhaoyan Meng, Bin Yi and Santasree Banerjee.

References

1. Dalal I, Tasher D, Somech R, Etzioni A, Garti BZ, Lev D, et al. Novel mutations in RAG1/2 and ADA genes in Israeli patients presenting with T-B-SCID or Omenn syndrome. Clin Immunol. 2011;140(3):284–90. https://doi.org/10.1016/j.clim.2011.04.011
2. Cirillo E, Giardino G, Gallo V, D'Assante R, Grasso F, Romano R, et al. Severe combined immunodeficiency-an update. Ann N Y Acad Sci. 2015;1356:90–106. https://doi.org/10.1111/nyas.12849
3. International union of immunological societies expert committee on primary immunodeficiencies, Primary immunodeficiencies: 2009 update. J Allergy Clin Immunol. 2009;124(6):1161–78. https://doi.org/10.1016/j.jaci.2009.10.013
4. Chinn IK, Shearer WT. Severe combined immunodeficiency disorders. Immunol Allergy Clin North Am. 2015;35(4):671–94. https://doi.org/10.1016/j.iac.2015.07.002
5. Van der Burg M, Ijspeert H, Verkaik NS, Turul T, Wiegant WW, Morotomi-yano K, et al. A DNA-PKcs mutation in a radiosensitive T-B- SCID patient inhibits Artemis activation and nonhomologous end-joining. J Clin Invest. 2008;119(1):91–8. https://doi.org/10.1172/JCI37141
6. Sharapova SO, Guryanova IE, Pashchenko OE, Kondratenko IV, Kostyuchenko IV, Rodina YA, et al. Molecular characteristics, clinical and immunologic manifestations of 11 children with Omenn syndrome in East Slavs (Russia, Belarus, Ukraine). J Clin Immunol. 2016;36(1):46–55. https://doi.org/10.1007/s10875-015-0216-7
7. Notarangelo LD, Kim MS, Walter JE, Lee YN. Human RAG mutations: biochemistry and clinical implications. Nat Rev Immunol. 2016;16(4):234–46. https://doi.org/10.1038/nri.2016.28
8. Cuperus E, Montfrans JMV, Gijn MEV, Bastiaens MT, Willigen MM, Lequit RJ, et al. Congenital erythroderma should be considered as an urgent warning sign of immunodeficiency: a case of Omenn syndrome. Eur J Dermatol. 2017;27(3):313–14. https://doi.org/10.1684/ejd.2017.2992
9. Shen J, Jiang L, Gao Y, Ou R, Yu S, Yang B, et al. A novel RAG1 mutation in a compound heterozygous status in a child with omenn syndrome. Front Genet. 2019;10:913. https://doi.org/10.3389/fgene.2019.00913
10. Fugmann SD, Lee AI, Shockett PE, Villey IJ, Schatz DG. The RAG proteins and V (D) J recombination: complexes, ends, and transposition. Annu Rev Immunol. 2000;18:495–527. https://doi.org/10.1146/annurev.immunol.18.1.495
11. Geier CB, Piller A, Linder A, Sauerwein KM, Eibl MM, Wolf HM. Leaky RAG deficiency in adult patients with impaired antibody production against bacterial polysaccharide antigens. PLoS One. 2015;10(7):e0133220. https://doi.org/10.1371/journal.pone.0133220
12. IJspeert H, Driessen GJ, Moorhouse MJ, Hartwig NG, Wolska-Kusnierz B, Kalwak K, et al. Similar recombination-activating gene (RAG) mutations result in similar immunobiological effects but in different clinical phenotypes. J Allergy Clin Immunol. 2014;133(4):1124–33. https://doi.org/10.1016/j.jaci.2013.11.028
13. Alt FW, Zhang Y, Meng FL, Guo C, Schwer B. Mechanisms of programmed DNA lesions and genomic instability in the immune system. Cell. 2013;152(3):417–29. https://doi.org/10.1016/j.cell.2013.01.007
14. Meshaal SS, El Hawary RE, Abd Elaziz D, Eldash A, Alkady R, Lotfy S, et al. Phenotypical heterogeneity in RAG-deficient patients from a highly consanguineous population. Clin Exp Immunol. 2019;195(2):202–12. https://doi.org/10.1111/cei.13222
15. Lee YN, Frugoni F, Dobbs K, Tirosh I, Du L, Ververs FA, et al. Characterization of T and B cell repertoire diversity in patients with RAG deficiency. Sci Immunol. 2016;1(6):eaah6109. https://doi.org/10.1126/sciimmunol.aah6109

16. Miao J, Ying B, Li R, Tollefson AE, Spencer JF, Wold WSM, et al. Characterization of an N-terminal non-core domain of RAG1 gene disrupted Syrian hamster model generated by CRISPR Cas9. Viruses. 2018;10(5):243. https://doi.org/10.3390/v10050243
17. Zhang R, Chen S, Han P, Chen F, Kuang S, Meng Z, et al. Whole exome sequencing identified a homozygous novel variant in CEP290 gene causes Meckel syndrome. J Cell Mol Med. 2020;24(2):1906-16. https://doi.org/10.1111/jcmm.14887
18. Richards S, Aziz N, Bale S, Bick D, Das S, Gastier-Foster J, et al. Standards and guidelines for the interpretation of sequence variants: a joint consensus recommendation of the American College of Medical Genetics and Genomics and the Association for Molecular Pathology. Genet Med. 2015;17(5):405-24. https://doi.org/10.1038/gim.2015.30
19. Schwarz JM, Cooper DN, Schuelke M, Seelow D. MutationTaster2: mutation prediction for the deep-sequencing age. Nat Methods. 2014;11(4):361-2. https://doi.org/10.1038/nmeth.2890
20. Omenn GS. Family reticuloendotheliosis with eosinophilia. N Engl J Med. 1965;273:427-32. https://doi.org/10.1056/NEJM196508192730806
21. Corneo B, Moshous D, Güngör T, Wulffraat N, Philippet P, Le Deist F, et al. Identical mutations in RAG1 or RAG2 genes leading to defective V (D) J recombinase activity can cause either TB-severe combined immune deficiency or Omenn syndrome. Blood. 2001;97(9):2772-6. https://doi.org/10.1182/blood.V97.9.2772
22. Schuetz C, Huck K, Gudowius S, Megahed M, Feyen O, Hubner B. et al. An immunodeficiency disease with rag mutations and granulomas. N Engl J Med. 2008;358(19):2030-8. https://doi.org/10.1056/NEJMoa073966
23. Lek M, Karczewski KJ, Minikel EV, Samocha KE, Banks E, Fennell T, et al. Analysis of protein-coding genetic variation in 60,706 humans. Nature. 2016;536(7616):285-91. https://doi.org/10.1038/nature19057
24. John T, Walter JE, Schuetz C, Chen K, Abraham RS, Bonfim C, et al. Unrelated hematopoietic cell transplantation in a patient with combined immunodeficiency with granulomatous disease and autoimmunity secondary to rag deficiency. J Clin Immunol. 2016;36(7):725-32. https://doi.org/10.1007/s10875-016-0326-x
25. Casanova JL, Conley ME, Seligman SJ, Abel L, Notarangelo LD. Guidelines for genetic studies in single patients: lessons from primary immunodeficiencies. J Exp Med. 2014;211(11):2137-49. https://doi.org/10.1084/jem.20140520
26. Chilosi M, Facchetti F, Notarangelo LD, Romaqnani S, Del PG, Almeriqoqna F, et al. CD30 cell expression and abnormal soluble CD30 serum accumulation in Omenn's syndrome: evidence for a T helper 2-mediated condition. Eur J Immunol. 1996;26(2):329-34. https://doi.org/10.1002/eji.1830260209
27. Zhang Z, Zhao X, Jiang L, Liu E, Cui Y, Wang M, et al. Clinical characteristics and molecular analysis of three Chinese children with Omenn syndrome. Pediatr Allergy Immunol. 2011;22(5):482-7. https://doi.org/10.1111/j.1399-3038.2010.01126.x
28. Anna S, Magdalena RZ, Monika K, Gruca A, Grabowska A, Lenart M, et al. Mutation c.256_257delAA in rag1 gene in Polish children with severe combined immunodeficiency: diversity of clinical manifestations. Arch Immunol Ther Exp. 2016;64(Suppl 1):177-83. https://doi.org/10.1007/s00005-016-0447-1
29. Khan TA, Iqbal A, Rahman H, Cabral MO, Ishfag M, Muhammad N. Novel rag1 mutation and the occurrence of mycobacterial and Chromobacterium violaceum infections in a case of leaky SCID. Microb Pathog. 2017;109:114-9. https://doi.org/10.1016/j.micpath.2017.05.033
30. Lawless D, Geier CB, Farmer JR, Allen HL, Thwaites D, Atschekzei F, et al. Prevalence and clinical challenges among adults with primary immunodeficiency and recombination-activating gene deficiency. J Allergy Clin Immunol. 2018;141(6):2303-6. https://doi.org/10.1016/j.jaci.2018.02.007
31. Picard C, Gaspar HB, Al-Herz W, Bousfiha A, Casanova J-L, Chatila T, et al. International union of immunological societies: 2017 primary immunodeficiency diseases committee report on inborn errors of immunity. J Clin Immunol. 2018;38(1):96-128. https://doi.org/10.1007/s10875-017-0464-9
32. Conley ME, Casanova JL. Discovery of single-gene inborn errors of immunity by next generation sequencing. Curr Opin Immunol. 2014;30:17-23. https://doi.org/10.1016/j.coi.2014.05.004
33. Ng SB, Buckingham KJ, Lee C, Bigham AW, Tabor HK, Dent KM, et al. Exome sequencing identifies the cause of a mendelian disorder. Nat Genet. 2010;42(1):30-5. https://doi.org/10.1038/ng.499
34. Dai Y, Liang S, Dong X, Zhao Y, Ren H, Guan Y, et al. Whole exome sequencing identified a novel DAG1 mutation in a patient with rare, mild and late age of onset muscular dystrophy-dystroglycanopathy. J Cell Mol Med. 2019;23(2):811-8. https://doi.org/10.1111/jcmm.13979

Supplementary

Table S1 Routine blood test report of the patient.

Test Project	08/04/2019	12/04/2019	15/04/2019	18/04/2019	21/04/2019	Reference	unit
leukocyte	4.36	2.42 ↓	2.29 ↓	2.26 ↓	2.58 ↓	4-11	10^9/L
Erythrocyte	4.6	3.8	3.6 ↓	3.2 ↓	3 ↓	3.8-5.8	10^{12}/L
Hemoglobin	116 ↓	94 ↓	89 ↓	78 ↓	71 ↓	117-174	g/L
Haematocrit	37.1	29.8 ↓	28.6 ↓	25.1 ↓	22.3 ↓	35-51	%
Mean corpuscular volume	80.7	79 ↓	79 ↓	78.7 ↓	75.1 ↓	80-100	fL
Mean corpuscular haemoglobin	25.2 ↓	24.9 ↓	24.6 ↓	24.5 ↓	23.9 ↓	27-35	pg
Mean erythrocyte haemoglobin concentration	313	315	311	311	318	310-370	g/L
Platelet count	769 ↑	599 ↑	711 ↑	645 ↑	631 ↑	100-300	10^9/L
Lymphocyte percentage	27.1	12 ↓	17.9 ↓	8 ↓	19.6 ↓	20-40	%
Monocyte percentage	12.4 ↑	3.7	5.7	18.1 ↑	1.9 ↓	3-8	%
Neutrophil percentage	58.9	76.9 ↑	67.7	58.9	60.7	50-70	%
Eosinophil percentage	0.5 ↓	6.6 ↑	7 ↑	2.7	7 ↑	1-3	%
Basophil percentage	0.2	0	0.4	0.4	0	0-1	%
Lymphocyte absolute value	1.18 ↓	0.29 ↓	0.41 ↓	0.18 ↓	0.31 ↓	1.5-4	10^9/L
Monocyte absolute value	0.54 ↑	0.09	0.13	0.41	0.03	0-0.45	10^9/L
Neutrophil absolute value	2.57	1.86 ↓	1.55 ↓	1.33 ↓	0.96 ↓	2-7	10^9/L
Eosinophil absolute value	0.02	0.16	0.16	0.06	0.11	0-0.45	10^9/L
Absolute value of basophil	0.01	0	0.01	0.01	0	0-0.02	10^9/L
Red blood cell distribution width (SD)	48.1 ↑	48.1 ↑	48.9 ↑	49.1 ↑	48.8 ↑	39-46	fL
Red blood cell distribution width (CV)	16.4 ↑	16.6 ↑	16.9 ↑	17 ↑	17.6 ↑	11.6-14	%
Platelet distribution width	11.2	11.5	10.4	10.3	10.3	9.8-17.2	fL
Average platelet volume	10.2	10.7	9.7	9.5	9.7	6.5-12	fL
Large platelet ratio	26	28.5	22.3	21.1	22.7	13-43	%
Platelet specific product	0.79	0.64	0.69	0.61	0.61		%
Naive granulocyte absolute value	0.04	0.02	0.03	0.27	0.17	0-0.06	
Naive granulocyte percentage	0.9 ↑	0.8 ↑	1.3 ↑	11.9 ↑	10.8 ↑	0-0.6	
Percentage of nucleated red blood cells		0	0	0	0		%
Absolute value of nucleated red blood cells		0	0	0	0		%
Serum amyloid		71.2 ↑	<5	87.52 ↑	78.59 ↑	0–10	mg/L

Table S2 Protein and Enzymatic Analysis of the patient.

Test Project	08/04/2019	12/04/2019	15/04/2019	18/04/2019	21/04/2019	Reference	Unit
Alanine aminotransferase	33.5	22.8	29.6	34	34.9	0-40	U/L
Aspartate aminotransferase	70.8 ↓	62.8 ↓	110 ↓	109.9 ↓	113.1 ↓	5-40	U/L
Asparagus	2.11	2.75	3.72	3.23	3.24	>1	
Total protein	61.4 ↓	49.3 ↓	50.8 ↓	54.1 ↓	56.7 ↓	66-87	g/L
albumin	38.6	30.3 ↓	31.7 ↓	27.3 ↓	30.3 ↓	35-55	g/L
globulin	22.8	19 ↓	19.1 ↓	26.8	26.4	20-40	g/L
White ball ratio	1.7	1.6	1.7	1 ↓	1.1	1.1-2.5	
Total bilirubin	5 ↓	2.5 ↓	2.6 ↓	2.9 ↓	1.9 ↓	5.1-25	μmol/L
Direct bilirubin	2		0.8	1.2	0.4	0-10	μmol/L
Indirect bilirubin	3		1.8 ↓	1.7 ↓	1.5 ↓	2-14	μmol/L
Alkaline phosphatase	130 ↑		101	83	78	39-117	U/L
Lactate dehydrogenase	383 ↑	433 ↑	927 ↑	619 ↑	598 ↑	114-245	U/L
γ-glutamyl transpeptidase	50		65 ↑	78 ↑	101 ↑	11-50	U/L
Determination of adenosine deaminase (ADA)	18.9		26.2	19.8	19.9		U/L
Creatine kinase	37 ↓	48 ↓	261	35 ↓	28 ↓	150-325	U/L
Creatine kinase isoenzyme	19.8	17.4	75 ↑	12.5	14.4	0-25	U/L
alpha-hydroxybutyrate dehydrogenase	320 ↑	352 ↑	774 ↑	509 ↑	484 ↑	72-182	U/L
glucose	5.73 ↑	4.95	4.23	5.87 ↑	5.1	3.33-5.55	mmol/L
Urea nitrogen	2	1.8	1.6	1.2	2		mmol/L
Creatinine	21 ↓	6 ↓	11 ↓	8 ↓	7 ↓	41-81	μmol/L
Uric acid	225	147 ↓	164 ↓	104 ↓	179 ↓	214-420	μmol/L
Determination of serum cystatin C	1.3	0.9	1.1	1	0.9		mg/L
Total cholesterol	1.86 ↓					3.4-6.5	mmol/L
Triglyceride	1.4					0.34-1.92	mmol/L
High density lipoprotein cholesterol	0.46 ↓					0.9-1.68	mmol/L
LDL cholesterol	0.71 ↓					1.9-3.8	mmol/L
Apolipoprotein A1	0.6 ↓					1.2-1.8	g/L
Glycolic acid	4.78		8.15 ↑	14.02 ↑	6 ↑	0.4-5	mg/L
Retinol binding protein	14.4 ↓	13.6 ↓	21.3 ↓	15.4 ↓	16.9 ↓	22-53	mg/L
Apolipoprotein B	0.5					0.5-1.5	g/L
calcium	2.21 ↑	2.06	2.06	2.03	2.07	2.1-2.75	mmol/L
phosphorus	1.24 ↓					1.5-2.2	mmol/L
iron	2.6 ↓					7-19	μmol/L
Zinc	4.42 ↓					7.72-21.4	μmol/L
magnesium	0.92					0.66-1.1	mmol/L
Potassium	4.71	4.73	5.75 ↑	4.44	4.08	3.5-5.5	mmol/L
sodium	136 ↑	132 ↓	135	134 ↓	136	135-145	mmol/L
chlorine	97	95 ↓	91 ↓	90 ↓	92 ↓	96-110	mmol/L
Amylase	16					0-200	U/L
Urea/creatinine	0.1	0.3 ↑	0.15	0.15	0.29 ↑	0.05-0.24	
CO2 binding	22.9	23.1	35 ↑	39.7 ↑	33.8 ↑	17.2-29	mmol/L
Immunoglobulin G	6.78		4.48			2.32-14.11	g/L
Immunoglobulin A	0		0			0-0.83	g/L
Immunoglobulin M	0.02 ↓		0.03 ↓			0.17-0.66	g/L
Procalcitonin (PCT) testing	1.2 ↑	8.02 ↑	1.44 ↑	1.86 ↑	0.94 ↑	0-0.5	ng/ml
Superoxide dismutase	109.9						U/ml
Calcium ion	1.1	1.03	1.03	1.01	1.03	0.9-1.4	mmol/L
Complement C3	1.5		1.25			0.8-1.6	g/L
Complement C4	0.47 ↑		0.45 ↑			0.1-0.4	g/L
C-reactive protein	31.25 ↑	16.55 ↑	8.16 ↑	22.36 ↑	16.73 ↑	0-5	mg/L
B-type brain natriuretic peptide precursor		100	100	150		0-300	pg/ml
Serum folic acid			26			3.89-26.8	ng/ml
Serum ferritin			537.3 ↑			25-200	ng/ml
Vitamin B12			807.4 ↑			100-700	pg/ml

Table S3 Immunopathological analysis of the patient.

Test Project	11/04/2019	15/04/2019	Reference	Unit
Total T cells (CD3+)	0 ↓	0 ↓	60.8-75.4	%
T helper cells (CD3+ **CD4+**)	0 ↓	0 ↓	29.4-45.8	%
T suppressor cells (CD3+ **CD8+**)	0 ↓	0 ↓	18.2-32.8	%
Total B cells (CD3− CD19+)	0 ↓	0 ↓	6-25	%
NK cells (CD3-CD16+ **CD56+**)	98 ↑	99 ↑	5-20	%
T helper cells/**T suppressor cells**	0 ↓	0 ↓	0.9-3.6	

Table S4 Amino acid analysis of the patient.

Test Project	12/04/2019	Reference
Alanine	150.63 ↓	172-1053
Arginine	7.47	2-44
Citrulline	6.43	6-52
Glycine	212.3	190-1255
Leucine	108.02	79-350
Methionine	17.9	6-34
Ornithine	50.61	28-318
Phenylalanine	62.4	24-100
Proline	106.18	95-418
Tyrosine	45.71	40-278
Valine	106.45	63-298
ARG/**ORN**	0.15	0.02-0.64
CIT/**ARG**	0.86	0.09-9.86
MET/**PHE**	0.29	0.07-4.11
ORN/**CIT**	7.87	0.95-16.13
PHE/**TYR**	1.37 ↑	0.18-1.09
TYR/**CIT**	7.11	0.02-21.9
ORN/**PHE**	0.81	0.15-4.83
LEU/**PHE**	1.73	0.49-6.88
GLY/**PHE**	3.4	4.19-20.39
Free carnitine	31	10.5-67.8
Acetyl Carnitine	31.56	1.3-39.3
Propionylcarnitine	0.96	0.3-4.95
C3DC-C4OH	0.21	0.02-0.36
Butyrylcarnitine	0.24	0.08-0.51
C4DC-C5OH	0.27	0.09-0.55
Isovalerylcarnitine	0.11	0.05-0.53
Prenylcarnitine	0.01	0.00-0.03
C5DC-C6OH	0.1	0.05-0.41
Hexanoylcarnitine	0.14 ↑	0.01-0.13
Adipylcarnitine	0.09	0.03-0.29
Octanoylcarnitine	0.09	0.01-0.14
Octenoylcarnitine	0.2	0.01-0.57
Decanoylcarnitine	0.11	0.02-0.19
Decenoylcarnitine	0.1	0.02-0.21
Decadienoylcarnitine	0.02	0.01-0.21
Dodecylcarnitine	0.07	0.02-0.22

(Continues)

Table S4 (continued)

Test Project	12/04/2019	Reference
Dodecenoylcarnitine	0.06	0.01-0.26
Myristyl carnitine	0.12	0.05-0.39
Myristyl carnitine	0.08	0.02-0.29
3-hydroxy-tetradecanoylcarnitine	0.01	0-0.03
Tetradecadienoylcarnitine	0.02	0.01-0.07
Cetyl carnitine	0.78	0.47-6.34
3-hydroxy-hexadecanoylcarnitine	0.03	0.01-0.05
Hexadecenoylcarnitine	0.09	0.02-0.39
3-hydroxy-hexadecenoylcarnitine	0.03	0.01-0.13
18 carbonyl carnitine	0.41	0.21-1.68
3-hydroxy-octadecanoylcarnitine	0.01	0-0.03
18 carbenoyl carnitine	1.38	0.39-2.75
3-hydroxy-octadecenoyl carnitine	0.02	0.01-0.06
18 carbon dienoyl carnitine	0.27	0.07-0.66
C3/C2	0.03 ↓	0.05-0.27
C4/C2	0.01	0-0.1
C5/C2	0	0-0.11
C8/C2	0	0-0.03
C14: 1/C16	0.1	0.01-0.21
C16-OH/C16	0.04 ↑	0-0.03
C14: 1/C8: 1	0.06	0.1-2.27
CO/ (C16+ C18)	26.05	2.56-48.97
C3/Met	0.07 ↓	0.12-1.99
C3/CO	0.03	0.01-0.15
C4/C3	0.25	0.04-0.38
C5/CO	0	0-0.02
C5/C3	0.11	0.03-0.51
(C3DC-C4OH) /C4	0.88	0.14-1.59
(C4DC-C5OH) /CO	0.01	0-0.02
(C4DC-C5OH) /C8	3	1.39-18.08
(C5DC-C6OH) /C8	1.11	0.83-14
C14: 1/C12: 1	0.15 ↑	0.01-0.12
C10/C8	0.82	0.38-2
C5DC-C6OH/C3	0	0-0.06
C16/C2	0.02 ↓	0.06-1.33
C16/C3	0.81	0.4-5.61
C18/C3	0.43	0.14-1.69
C18OH/C3	0.01	0-0.03

Table S5 Clotting factor analysis of the patient.

Test Project	09/04/2019	12/04/2019	References	Unit
Prothrombin time	34.7 ↑	11.6	0–14	s
Prothrombin time activity	21.9 ↓	108.6	70–130	%
Prothrombin time ratio	3.04 ↑	0.97	0.85–1.15	
International normalized ratio of prothrombin time	3.04 ↑	0.97	0.8–1.5	
Activated partial prothrombin time	80 ↑	52.8 ↑	22–40	s
Fibrinogen assay	2.78	2.46	2–6	g/L
Thrombin time determination	>60 ↑	24.1	11–25	s

Table S6 Hepatitis antigen-antibody analysis for the patient.

Test Project	09/04/2019
Hepatitis B surface antigen	Negative (−)
Hepatitis B surface antibody	Positive (+)
Hepatitis B e antigen	Negative (−)
Hepatitis B e antibody	Negative (−)
Hepatitis B core antibody	Negative (−)
Pre-si antigen of hepatitis B virus outer membrane protein	Negative (−)
Hepatitis C antibody	Negative (−)
Hepatitis E antibody	Negative (−)
AIDS antibody	Negative (−)
Treponema pallidum antibody	Negative (−)

Table S7 Virus and bacterial study of the patient.

Test Project	09/04/2019
Parainfluenza virus IgM antibody	Negative (−)
Syncytial virus IgM antibody	Negative (−)
Mycoplasma pneumoniae IgM antibody	Negative (−)
Chlamydia pneumoniae IgM antibody	Negative (−)
Adenovirus antibody assay	Negative (−)
Influenza virus antibody assay	Negative (−)

Table S8 Bacterial and fungal culture analysis of the patient.

Test Project	09/04/2019	10/04/2019	16/04/2019
Bacterial culture and identification	See normal respiratory bacteria	No bacterial growth	See normal respiratory bacteria
Fungal culture identification	Candida albicans	No fungal growth	No fungal growth

Table S9 Bacterial DNA study in the patient.

Test Project	11/04/2019	15/04/2019	Reference
Mycoplasma pneumoniae-DNA	Negative (−)	Negative (−)	Negative
Chlamydia pneumoniae-DNA	Negative (−)	Negative (−)	Negative
Mycobacterium tuberculosis-DNA	Negative (−)	Negative (−)	Negative
Streptococcus pneumoniae DNA	Negative (−)	Negative (−)	Negative
Staphylococcus aureus DNA	Negative (−)	Negative (−)	Negative
Escherichia coli DNA	Negative (−)	Negative (−)	Negative
Klebsiella pneumoniae DNA	Negative (−)	Negative (−)	Negative
Pseudomonas aeruginosa DNA	Negative (−)	Negative (−)	Negative
Acinetobacter baumannii DNA	Negative (−)	Negative (−)	Negative
Stenotrophomonas maltophilia DNA	Negative (−)	Negative (−)	Negative
Haemophilus influenzae DNA	Negative (−)	Negative (−)	Negative
Legionella pneumophila DNA	Negative (−)	Negative (−)	Negative
Methicillin-resistant Staphylococcus DNA	Positive (+)	Positive (+)	Negative
Mycobacterium tuberculosis complex DNA	Negative (−)	Negative (−)	Negative

Table S10 Cellular immunoassay of the patient.

Test Project	12/04/2019
No stimulation (N)	0.03
Non-specific gamma interferon (P)	0.02
Specific gamma interferon (T)	0.02
(T-N) / **(P-N)**	0.2
Mycobacterium tuberculosis specific cellular immunoassay	Negative

Table S11 G-experiment and endotoxin test for the patient.

Test Project	15/04/2019	Reference	Unit
G experiment	58.47	<70	pg/ml
GM experiment	0.52	<0.65	ug/ml
Endotoxin test	0.06	<0.08	EU/ml

Table S12 Blood grouping of the patient.

Test Project	22/04/2019	22/04/2019
ABO blood type	O type	O type
RH blood type	Positive	Positive
ABO blood type (negative)		O type
Irregular antibody screening		negative

Table S13 Physical and chemical characteristics of patient's blood and urine.

Test Project	13/04/2019	Reference	Unit
pH	6.5	5.4-8.4	
proportion	1.005	1-1.03	
protein	negative	negative	g/L
glucose	negative	negative	mmol/L
Ketone body	negative	negative	mg/L
Bilirubin	negative		μmol/L
Urobilinogen	normal		μmol/L
Nitrite	negative	negative	
Urine leukocyte	negative	negative	leu/μl
Occult blood	negative	negative	mg/l
ascorbic acid	negative		mmol/L
colour	Light yellow		
transparency	Clear		
leukocyte	13 ↑	0–11	μL
Leukocyte mass	—	0-2	/μl
Atypical red blood cells	—		%
Erythrocyte	1	0-9	μL
Squamous epithelium	—	0-11	/μl
Renal epithelium	—	0-6	/μl
Oval fat body	—	0-2	/μl
Mucus	—	0-480	/μl
Transparent tube type	—	0-2	/LPF
Granular cast	—	0-1	/LPF
Erythrocyte cast	—	0-1	/LPF
Leukocyte cast	—	0-1	/LPF
Epithelial cell cast	—	0-1	/LPF
Cell cast	—	0-1	/LPF
Wide tube type	—	0-1	/LPF
Fat tube type	—	0-1	/LPF
Wax type	—	0-1	/LPF
Unclassified cast	—	0-2	/LPF
Calcium oxalate crystal	—	0-3	/HPF
Calcium phosphate crystal	—	0-3	/HPF
Calcium carbonate crystals	—	0-3	/HPF
Urate Crystal	—	0-3	/HPF
Unclassified crystal	—	0-10	/HPF

Table S14 Stool culture of the patient.

Test Project	14/04/2019	Reference	Unit
Stool color	yellow		
Fecal traits	Soft stool		
leukocyte	Not seen	0-3	Unit/HP
Erythrocyte	Not seen	0	Unit /HP
Fecal occult blood	Negative (−)	negative	
Fat ball	Not seen	Not seen	Unit /HP
phagocyte	Not seen	Not seen	Unit /HP
Pus cell	Not seen	Not seen	Unit /HP
Starch granules	Not seen	Not seen	Unit /HP
Yeast-like bacteria	Not seen	Not seen	Unit /HP
Intestinal mucosal epithelial cells	Negative (−)	Not seen	Unit /HP
Plant cell	Not seen	Not seen	Unit /HP
Fungus	Not seen	Not seen	Unit /HP
Pinworm eggs	Not seen	Not seen	Unit /HP
Roundworm eggs	Not seen	Not seen	Unit /HP
Whipworm eggs	Not seen	Not seen	Unit /HP
Taenia solium	Not seen	Not seen	Unit /HP
protozoan	Not seen	Not seen	Unit /HP
Muscle **fibre**	Not seen	Not seen	Unit /HP
Connective tissue	Not seen	Not seen	Unit /HP